Supplementary Information

Shaoting Lin[†1], *Tal Cohen*[†2,3], *Teng Zhang*[†1,4], *Hyunwoo Yuk*[1], *Rohan Abeyaratne*[1], *Xuanhe Zhao*[1,3*]

1. Department of Mechanical Engineering, Massachusetts Institute of Technology, Cambridge, MA 02139;
2. School of Engineering and Applied Science, Harvard University, Cambridge, MA 02138;
3. Department of Civil and Environmental Engineering, Massachusetts Institute of Technology, Cambridge, MA 02139; 4. Department of Mechanical Engineering, Syracuse University, Syracuse, NY 13244;
†. These authors contribute equally to this paper; * To whom correspondence should be addressed.
Email: zhaox@mit.edu

This PDF file includes:

Theoretical model

Supplementary Figures S1 to S9

Captions for Supplementary Videos S1 to S3

Problem setting. Consider a semi-infinite incompressible elastic strip with a rectangular cross-section as illustrated on Fig. S9. A material particle in the layer is labeled by its coordinates (X, Y, Z) in the undeformed state. The undeformed width of the specimen is W and its hight H such that the strip occupies the region

$$-W/2 < X < W/2, \quad -\infty < Y < \infty, \quad -H/2 < Z < H/2. \tag{1}$$

The top and bottom surfaces of the strip (at $Z = \pm H/2$) are perfectly adhered to rigid plates while the sides (at $X = \pm W/2$) are traction free. As the rigid plates are drawn away from each other the specimen is stretched to the new deformed thickness h, while the free surfaces retreat to form a meniscus shape to comply with the incompressibility constraint. We denote the spatial coordinate system in the deformed configuration by (x, y, z) and by limiting the analysis to plane-strain deformation patterns we have $y = Y$. Therefore, in the deformed state, the specimen occupies the range

$$-\frac{W}{2}\lambda_X \leqslant x \leqslant \frac{W}{2}\lambda_X, \quad -\infty < y < \infty, \quad -h/2 \leqslant z \leqslant h/2, \tag{2}$$

where $\lambda_X(Z)$ represents the in-plane stretch of the layer in the X-direction and as such is the normalized meniscus shape which we attempt to find in the present analysis. Here we have anticipated the fact that λ_X is independent of X, a fact that is established below.

Horizontal planes remain planes. The only additional assumption made about the deformation field of the specimen under tensile deformation, is that any horizontal plane in the unloaded state, remains planar and horizontal upon deformation. This assumption was employed in previous studies [1] and, intuitively, is motivated by the fact that both the midplane and the constrained planes necessarily remain planar. Our numerical simulations indicate that this is a good approximation and is not compromised even as the extension progresses and, in fact, the opposite tendency is observed. Note that in compression this assumption holds only in the small strains regime and thus the present study, in pursuit of the large strains response, is limited to tension.

Constitutive response. In the present study we employ the neo-Hookean constitutive model which can be written in terms of the elastic strain energy density per unit volume of undeformed material, in the form

$$\Psi = \frac{\mu}{2}\left(\mathrm{tr}(\mathbf{F}\mathbf{F}^{\mathrm{T}}) - 3\right), \tag{3}$$

where μ is the shear modulus and $\mathbf{F}$ is the deformation gradient which, for incompressible materials must obey the constraint

$$\det \mathbf{F} = 1. \tag{4}$$

Formulation. Since planes of constant Z are taken to remain planar upon deformation, the vertical coordinate z of any material point depends only on its initial vertical location Z while the in-plane coordinate x may depend on both X and Z. Hence we write the location of a material particle in the deformed configuration in the most general form as

$$x = g(X, Z), \quad y = Y, \quad z = f(Z). \tag{5}$$

Considering perfect adhesion of the specimens to the plates with no rigid motion, we write the boundary conditions

$$f(0) = 0, \quad f(\pm H/2) = \pm h/2, \quad g(0, Z) = 0, \quad g(X, \pm H/2) = X. \tag{6}$$

The deformation gradient $\mathbf{F}$ and the stretch λ_X can now be written in the form

$$\mathbf{F} = \begin{bmatrix} \frac{\partial g}{\partial X} & 0 & \frac{\partial g}{\partial Z} \\ 0 & 1 & 0 \\ 0 & 0 & f' \end{bmatrix}, \quad \lambda_X = \frac{\partial g}{\partial X}, \tag{7}$$

where the prime denotes differentiation with respect to Z. The incompressibility condition in (4) yields the differential equation

$$\frac{\partial g}{\partial X} = \frac{1}{f'} = \lambda_X. \tag{8}$$

Since f is a function of Z alone, it now follows that so is the stretch λ_X. By integrating the above equation and using the boundary condition $(6)^3$ we arrive at the relation

$$g(X,Z) = X\lambda_X. \tag{9}$$

We now insert the relations for g and f in terms of the meniscus shape λ_X back into $(7)^1$ to write

$$\mathbf{F} = \begin{bmatrix} \lambda_X & 0 & X\lambda_X' \\ 0 & 1 & 0 \\ 0 & 0 & 1/\lambda_X \end{bmatrix}. \tag{10}$$

Hence, for the class of deformations at hand, the problem reduces to finding a single unknown function $\lambda_X(Z)$ with the remaining boundary conditions translated to the form

$$\lambda_X(\pm H/2) = 1, \quad \lambda_X'(0) = 0, \quad \lambda = \int_0^{H/2} \frac{2}{\lambda_X H} dZ\ , \tag{11}$$

where the second condition is due to symmetry and the specimen stretch is $\lambda = h/H$.

Since the boundary conditions on the traction-free side-surfaces cannot be identically satisfied, we seek a deformation field that minimizes the elastic energy in the system within the class of deformations being considered. The total elastic energy stored in the system is obtained by integrating the energy density (3) over the cross-section of the specimen, which upon inserting the deformation gradient in (10), can be written as

$$E = 2\mu \int_0^{H/2} \int_0^{W/2} \left(2 - \lambda_X^2 - \lambda_X^{-2} - X^2(\lambda_X')^2\right) dXdZ, \tag{12}$$

where we have taken advantage of symmetry. This can be simplified by integration over X:

$$E = \mu W \int_0^{H/2} \left(2 - \lambda_X^2 - \lambda_X^{-2} - \frac{1}{3}\left(\frac{W}{2}\right)^2 (\lambda_X')^2\right) dZ - \frac{\mu W C}{6}\left(\int_0^{H/2} \frac{dZ}{\lambda_X} - \frac{h}{2}\right), \tag{13}$$

where the second term incorporates the displacement constraint $(11)^3$ with the Lagrange multiplier C.

To find a function λ_X which minimizes the total energy, we begin by calculating the first variation of the elastic energy E

$$\delta E = 2\mu W \int_0^{H/2} \left(\left(\lambda_X^{-3} + \frac{C}{6}\lambda_X^{-2} - \lambda_X\right)\delta\lambda_X - \frac{1}{3}\left(\frac{W}{2}\right)^2 \lambda_X'\delta\lambda_X'\right) dZ. \tag{14}$$

This can be further simplified via integration by parts to write

$$\delta E = 2\mu W \int_0^{H/2} \left(\lambda_X^{-3} + \frac{C}{6}\lambda_X^{-2} - \lambda_X + \frac{1}{3}\left(\frac{W}{2}\right)^2 \lambda_X''\right) \delta\lambda_X dZ - \cancel{\frac{2\mu W}{3}\left(\frac{W}{2}\right)^2 [\lambda_X'\delta\lambda_X]_0^{\frac{H}{2}}}\ , \tag{15}$$

where, since λ_X is prescribed at $Z = \pm H/2$, we require its variation to vanish there. Moreover the slope λ_X' vanishes at $Z = 0$ according to (11). Therefore the last term in the above relation cancels out and the vanishing of the first variation, $\delta E = 0$, requires

$$\left(\frac{W}{2}\right)^2 \lambda_X'' = 3\lambda_X - \frac{C}{2}\lambda_X^{-2} - 3\lambda_X^{-3}. \tag{16}$$

This can integrated after replacing $\lambda_X'' = \frac{\partial \lambda_X'}{\partial \lambda_X}\lambda_X'$, to arrive at a separable equation which by integration reads

$$\frac{W}{2}\lambda_X' = \left(3\lambda_X^2 + C\lambda_X^{-1} + 3\lambda_X^{-2} + D\right)^{1/2}, \tag{17}$$

where D is an integration constant. Here, in taking the square root, we have chosen the physically relevant branch with positive slope in the midplane. It is instructive to notice from (16) with $\lambda_X = 1$ that the coefficient C is proportional to the curvature of the meniscus shape near the constrained surfaces.

Numerical solution of the above nonlinear differential equation can be obtained by straight forward integration as conducted in the present study via the Runge-Kutta Merson method. To account for all three boundary conditions (11), a shooting method is applied in which the value of C is guessed to iteratively arrive at the required stretch ($\lambda = h/H$). Specifically for the first order equation (17), it is convenient to apply the symmetry boundary condition by defining the in-plane stretch in the midplane by

$$\lambda_X(Z=0) = \lambda_{X0}, \tag{18}$$

and thus via $(11)^2$ it is possible to eliminate D from (17) to write

$$\frac{W}{2}\lambda_X' = \left(3(\lambda_X^2 - \lambda_{X0}^2) + C(\lambda_X^{-1} - \lambda_{X0}^{-1}) + 3(\lambda_X^{-2} - \lambda_{X0}^{-2})\right)^{1/2}. \tag{19}$$

A shooting method can then be applied to relate the midplane stretch λ_{X0} to the specimen stretch h/H.

The applied stress. After carrying out the analysis of the previous section, we can insert the deformation field characterized by the single function $\lambda_X(Z)$ back into the energy integral in (12). This allows us to express the stored elastic energy (per unit length) as a function of the specimen's deformed thickness $E = E(h)$. The increment of work (per unit length) invested by the nominal averaged nominal stress S acting on the plates is $WS\delta h$ and this must equal the increment in energy δE:

$$\delta E = WS\delta h, \tag{20}$$

therefore we may write

$$S = \frac{1}{W}\frac{dE}{dh} = \frac{1}{WH}\frac{dE}{d\lambda}, \tag{21}$$

and hence we arrive at the stress-stretch relationship $S = S(\lambda)$.

Figures and Figure Captions

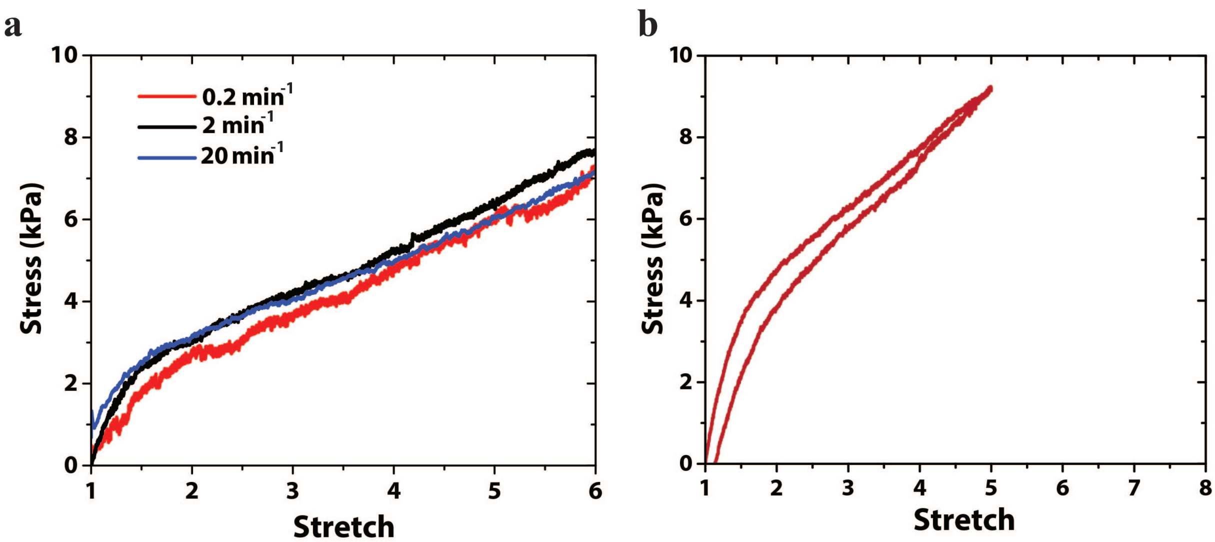

FIG. S1: **(a)** Monotonic loading at various loading rates; **(b)** Cyclic loading at the rate of 2 min^{-1}.

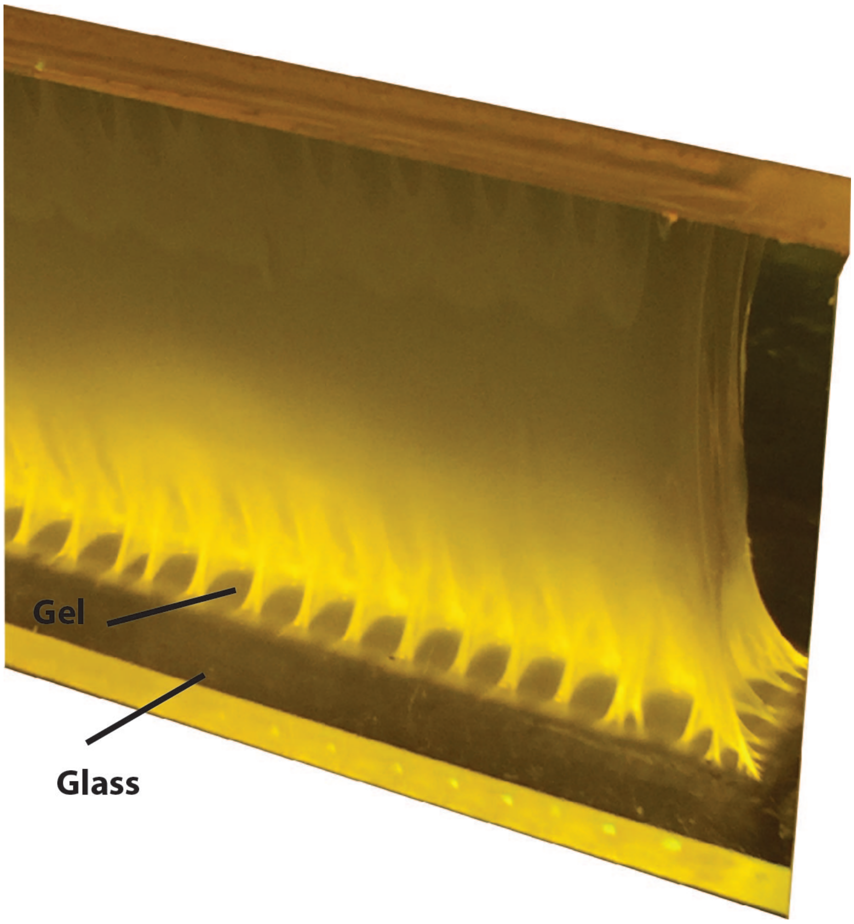

FIG. S2: Fluorescent image of the narrow sample under high deformation with fringe instability forming at the edge. Hydrogel sample with Rhodamine B added is stretched severely. Fringe instability forms at the fixed edge. The fluorescent light in the bounded surface shows the whitish material remaining on the surface, demonstrating perfect interfacial bonding between hydrogel and rigid substrate.

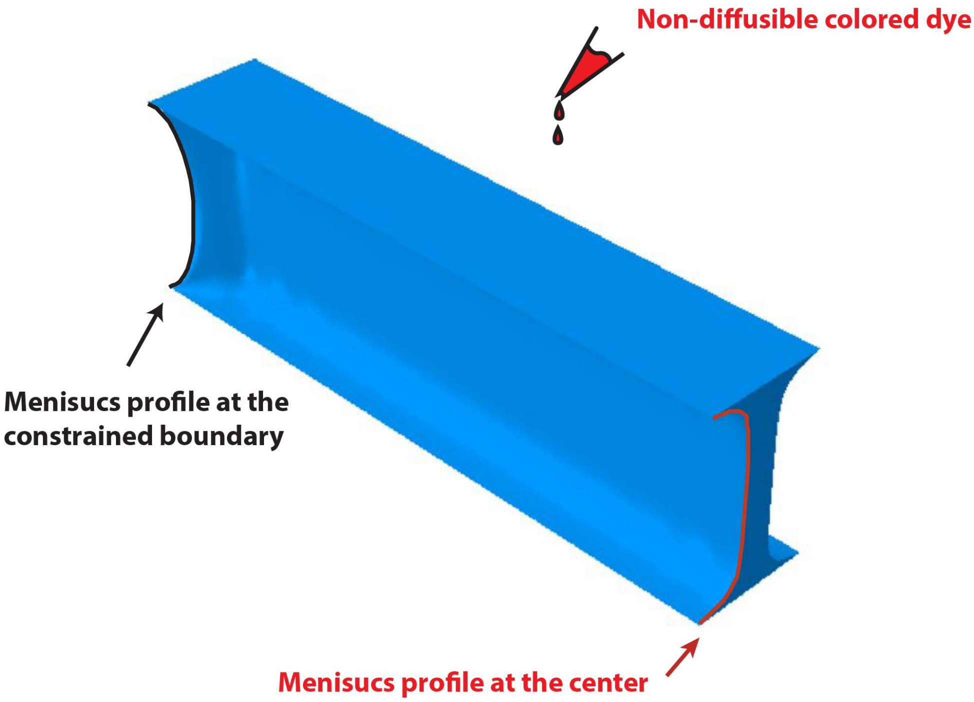

FIG. S3: Non-diffusible colored dye is covered on the surface of transparent hydrogel sample to distinguish with the meniscus profile at the constrained boundary.

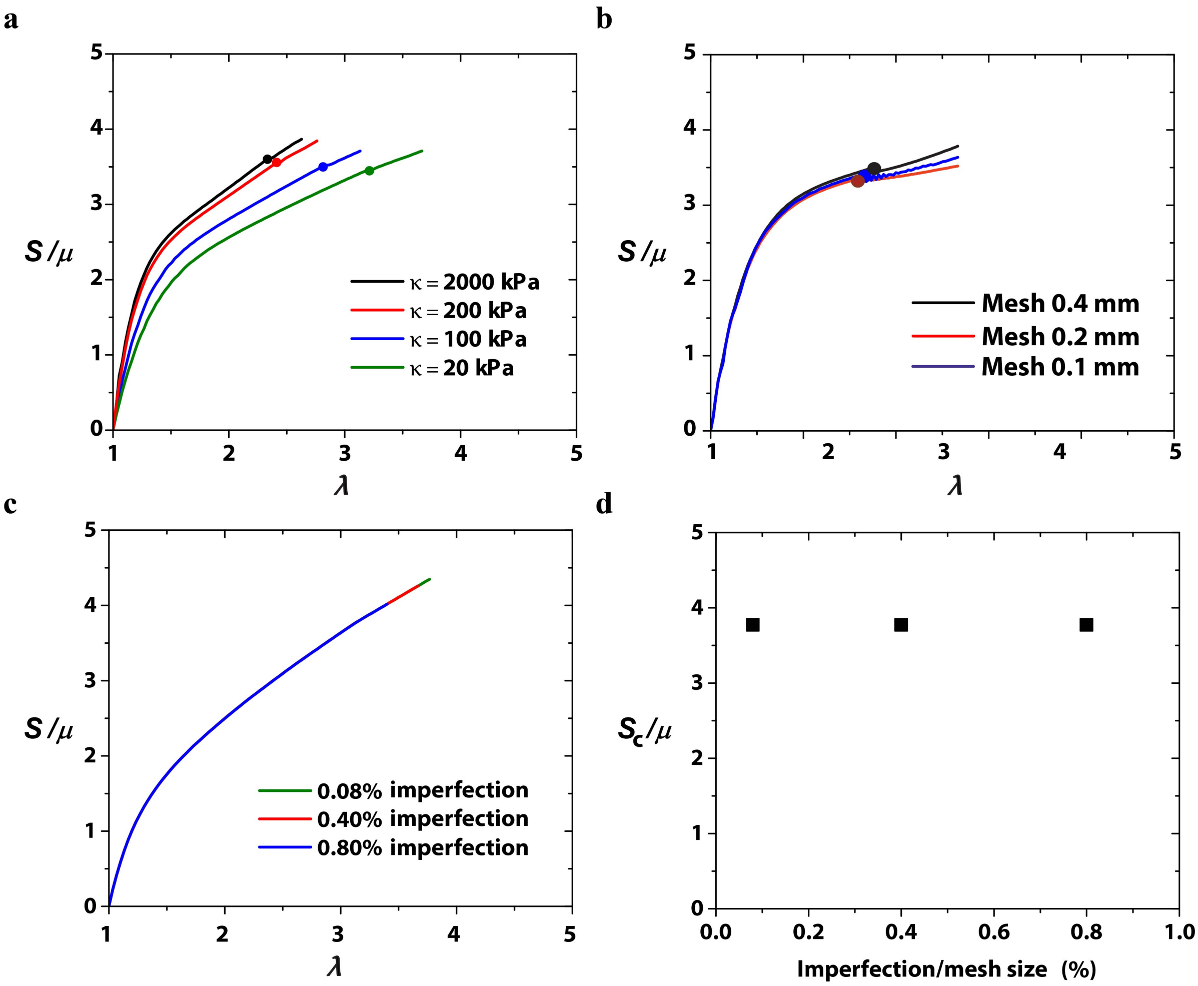

FIG. S4: **(a)** The nominal stress-stretch curve for the sample with W/H=3.2 of various bulk modulus; **(b)** The nominal stress-stretch curve for the sample with W/H=4 of various mesh size; **(c)** The nominal stress-stretch curve for the sample with W/H=2 of various ratios of imperfection to mesh size; **(d)** The critical stress for the sample with W/H=2 of various ratios of imperfection to mesh size.

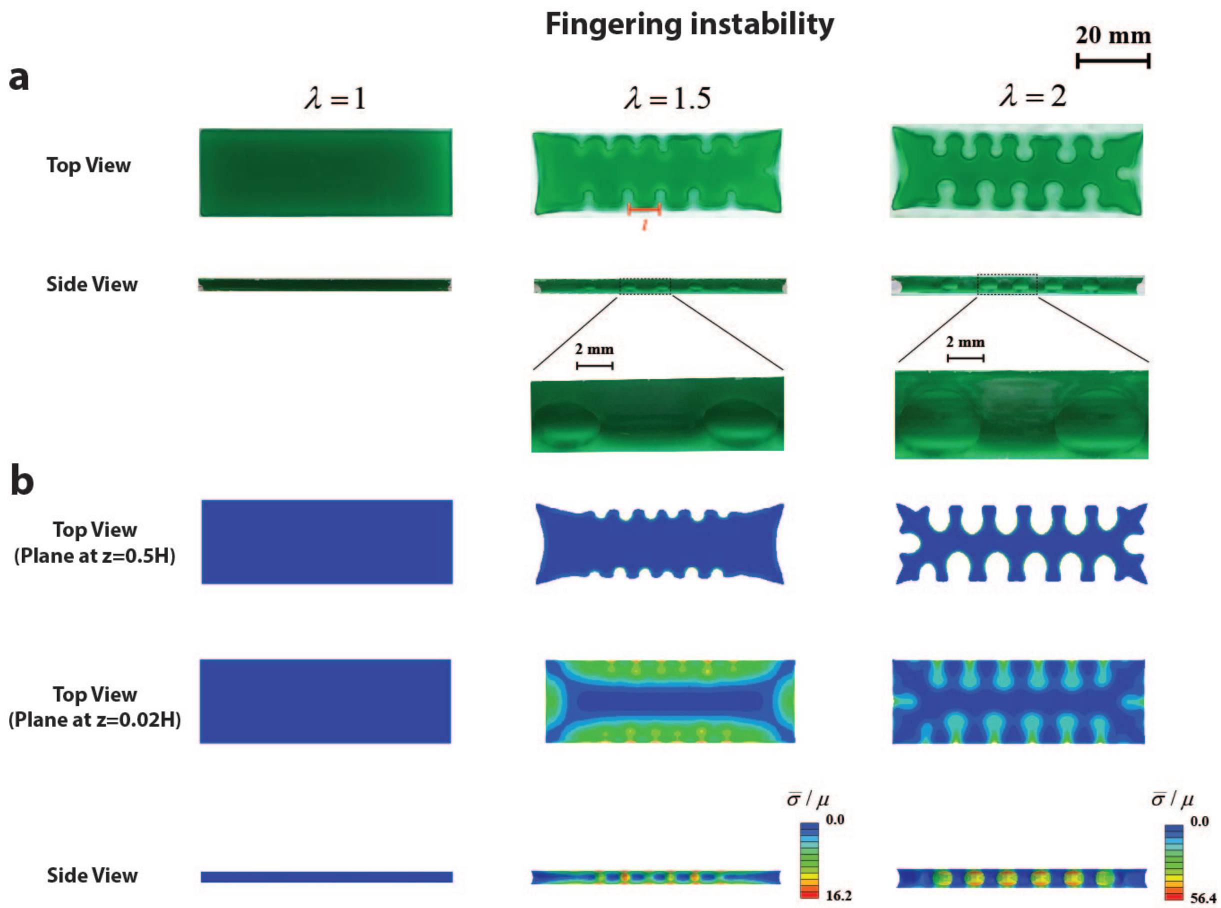

FIG. S5: **(a)** Experimental observation of the formation of fingering instability for sample with the width-thickness ratio of 2 as strain increases; **(b)** Numerical simulation of the formation of fingering instability for a sample with identical dimension.

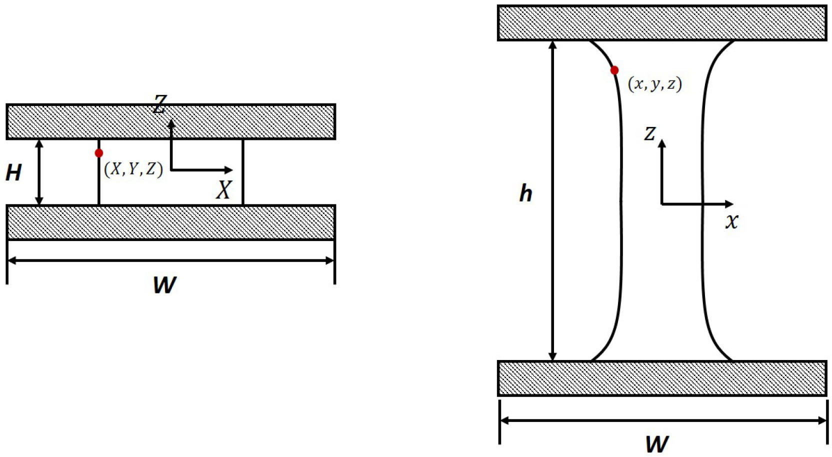

FIG. S6: The cross-section of the specimen in deformed and un-deformed.

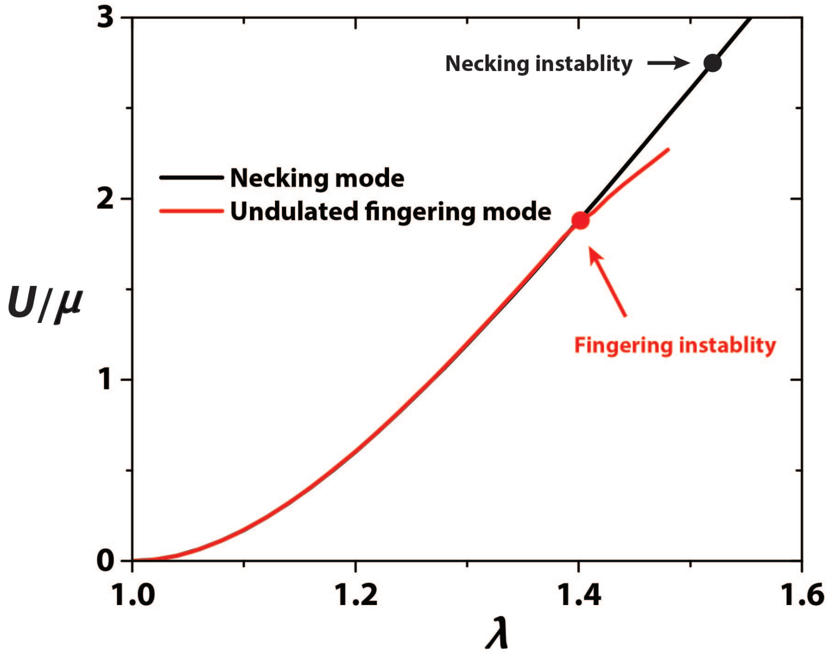

FIG. S7: Comparison of the elastic energy between necking mode and undulated fingering mode for the sample with W/H = 8.

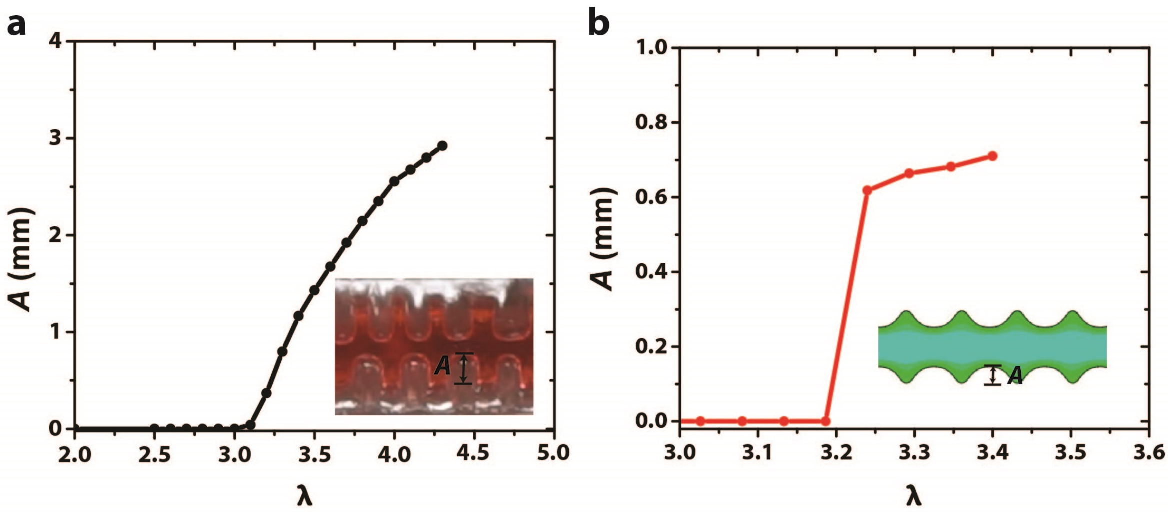

FIG. S8: Amplitude versus imposed stretch for the sample with $W/H = 2$.**(a)** Measured in experiment; **(b)** Measured in simulation.

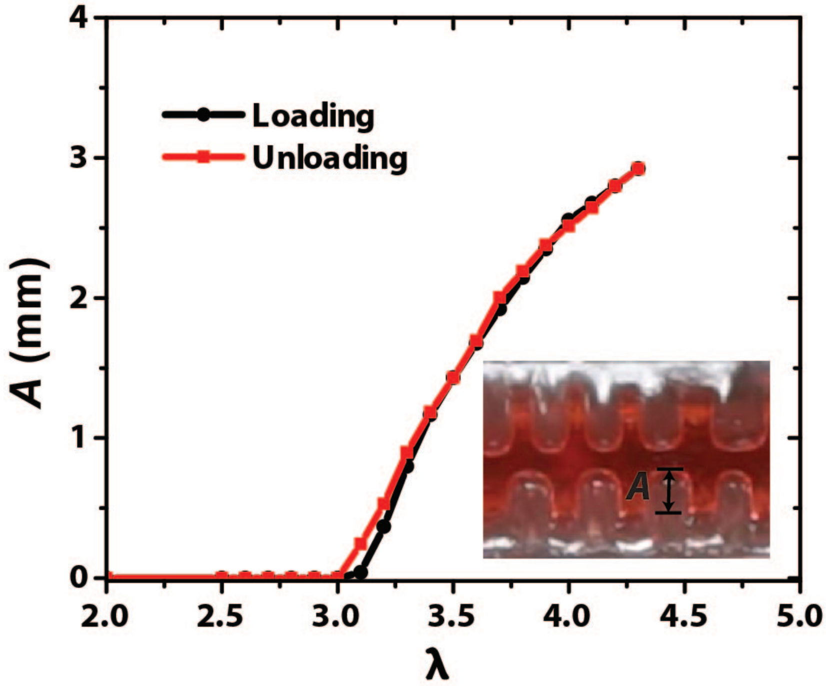

FIG. S9: Loading-unloading curve of amplitude versus imposed stretch for the sample with $W/H = 2$.

Captions for Supplementary Videos

Supplementary Videos S1

Top view and side view of the formation of the fringe instability for the sample with $W/H = 2$.

Supplementary Videos S2

Simulation of the formation of the fringe instability for the sample with $W/H = 2$.

Supplementary Videos S3

Top view and side view of the formation of the fingering instability for the sample with $W/H = 8$.

[1] Werner W Klingbeil and Richard T Shield. Large-deformation analyses of bonded elastic mounts. *Zeitschrift für angewandte Mathematik und Physik ZAMP*, 17(2):281–305, 1966.